

# Segmentation-Based Quantitation of Pulmonary Alveolar Proteinosis, Pre- and Post-Lavage, Using High-Resolution Computed Tomography

Tessa Sundaram Cook<sup>1</sup>, Nicholas Tustison<sup>1</sup>, Gang Song<sup>2</sup>, Suyash Awate<sup>1</sup>,  
Drew A. Torigian<sup>1</sup>, Warren Geftter<sup>1</sup>, and James C. Gee<sup>1</sup>

<sup>1</sup> Dept. of Radiology, Hospital of the University of PA, USA

<sup>2</sup> Dept. of Computer Science, University of Pennsylvania, USA

**Abstract.** Pulmonary alveolar proteinosis is a disorder of surfactant deposition that leads to the accumulation of lipoproteinaceous material in the alveoli. The mainstay of treatment is whole-lung lavage, by which saline is used to wash the alveolar deposits from the lung. Patients are currently followed using sequential pre- and post-lavage CT to subjectively assess treatment efficacy. We present an approach to quantify global and regional changes in disease distribution before and after lavage using automated and semiautomated segmentation methods. Histogram analysis demonstrates a leftward shift in parenchymal intensities after lavage, reflecting an increase in the degree of aerated lung after removal of excess surfactant. This methodology can be applied to a variety of pulmonary pathologies that manifest as a combination of alveolar and interstitial disease, to enable more quantitative assessment of disease progression and treatment efficacy.

## 1 Introduction

Pulmonary alveolar proteinosis (PAP) is a rare but potentially devastating condition in which lipoproteinaceous deposits accumulate in the alveoli as a result of impaired surfactant clearance, [1]. Congenital, idiopathic and acquired forms exist, and recent studies have linked PAP to a relative deficiency of granulocyte-macrophage colony stimulating factor (GM-CSF), a substance thought to activate alveolar macrophages [2]. However, pharmacologic treatment for PAP remains an active area of research. Currently, the mainstay of treatment is whole-lung lavage (WLL), which is performed under general anesthesia and involves sequentially washing out one lung with many liters of normal saline while ventilating the other, [3]. Multiple treatments are often required over a patient's lifetime, as alveolar deposits build up between treatments, and pneumonia with atypical organisms can cause death in these patients.

Computed tomography (CT) has been used to qualitatively assess the success of WLL. PAP has traditionally been associated with the "crazy paving" pattern of thickened interlobular septa and ground glass opacification, [4], although findings span the spectrum from alveolar predominance to interstitial fibrosis, [5].

Evaluation of CT studies by radiologists typically involves visually estimating a global increase or decrease in the volume of diseased lung. Reports of these studies generally assess the extent of disease as “same”, “worse” or “better”.

We present an approach toward quantifying the effects of whole-lung lavage in the treatment of pulmonary alveolar proteinosis. Using a combination of automated and semiautomated segmentation, we estimate the volume of lung parenchyma affected by disease and quantify both global and lobar effects of lung lavage on five patients with PAP. Our approach is an initial step toward an objective assessment of the efficacy of WLL—an improvement upon subjective interpretations currently used in clinical practice by radiologists.

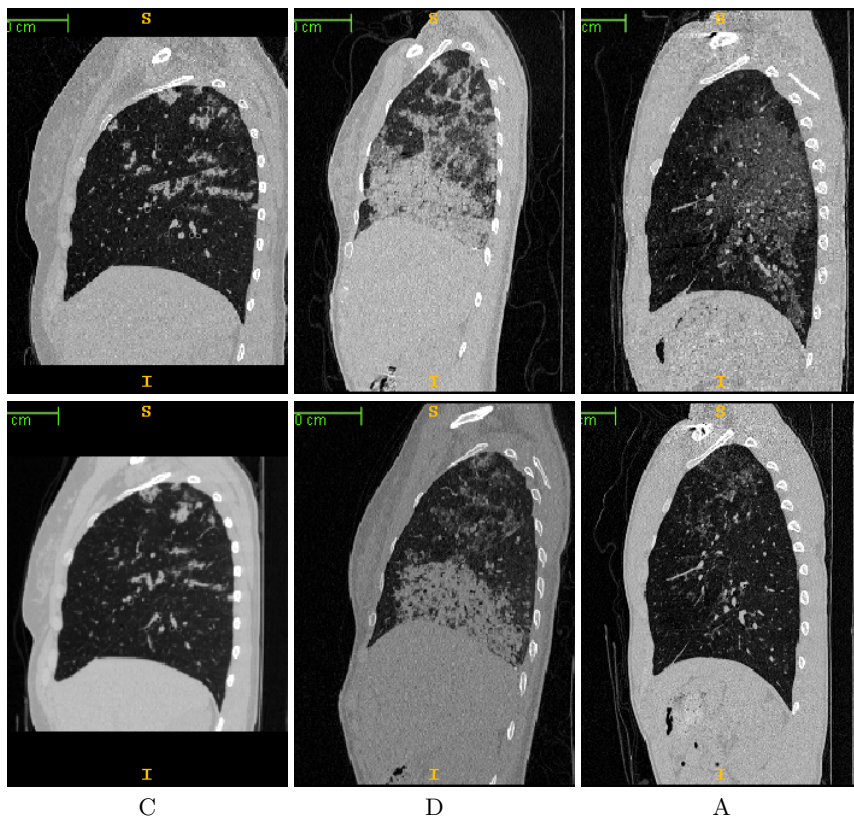


**Fig. 1.** Sagittal sections pre- (top) and post-lavage (bottom) show examples of lung involvement in three individuals, patients A, C and D. In some patients (e.g., A and D), lavage can be extremely effective, while in others (e.g., C) there is not much difference between the pre- and post-treatment images.

## 2 Materials and Methods

The complete analysis algorithm is illustrated in figure 2, using representative coronal CT sections from patient A both before and after treatment with whole-lung lavage. In the sections that follow, the terms “intensity” and “CT attenuation” are used interchangeably.

### 2.1 Data

High-resolution CT (HRCT) scans from five patients (designated A–E) with pulmonary alveolar proteinosis obtained immediately prior to and several months after WLL were selected for analysis. The pre- to post-lavage imaging interval ranged from 2 weeks to 12 months. The data were acquired with a matrix of  $512 \times 512$  and sub-millimeter slice thicknesses. To stay within the memory limitations of our image registration algorithm (applied in the next section), images are resampled to dimensions of  $256 \times 256 \times N$ , where  $N$  is the number of slices required to achieve isotropic voxels. Figure 1 shows sagittal sections pre- and post-lavage in three patients used in this experiment.

### 2.2 Whole-Lung and Lobar Segmentation

The pre-lavage images are segmented using an automated segmentation pipeline, implemented in the open-source Insight Toolkit, [6], that employs the methodology of Hu et al, [7]. First, an optimal threshold is calculated to separate the airways and lungs from the rest of the body. Whereas in [7] an iterative approach is used, we achieve better results more quickly using Otsu thresholding. Following the segmentation of the lungs and airways from the body, we isolate the trachea from a proximal axial slice using a Hough transform of the region of interest. We then iterate through subsequent slices to segment the remainder of the trachea by propagating the solution at the previous slice to the current slice. This iterative process stops once we have propagated the solution into both the left and right lungs, yielding the segmentation of three anatomic regions of interest (trachea, left lung, right lung). Finally, smoothing of the segmentation is performed using a specific ordering of binary morphological operations as suggested in [7].

Lobar segmentation follows in a semi-automated fashion using ITK-SNAP,[8]. The active contours are initialized using edge-based parameters rather than intensity-based thresholds, and segmentation is advanced in a stepwise fashion to generate a gross approximation of a particular lung lobe. Manual editing using the knife and polygon tools is then used to complete the segmentation.

The post-lavage images are segmented by registration of the pre- and post-lavage images and warping of the pre-lavage segmentation into the domain of the post-lavage image. For registration, we use the open-source Advanced Normalization Tools (ANTs), [9], which offer several similarity metrics and both linear and non-linear transformation options for accurate modeling of biomechanical deformations. For the experiments discussed in this paper we use the

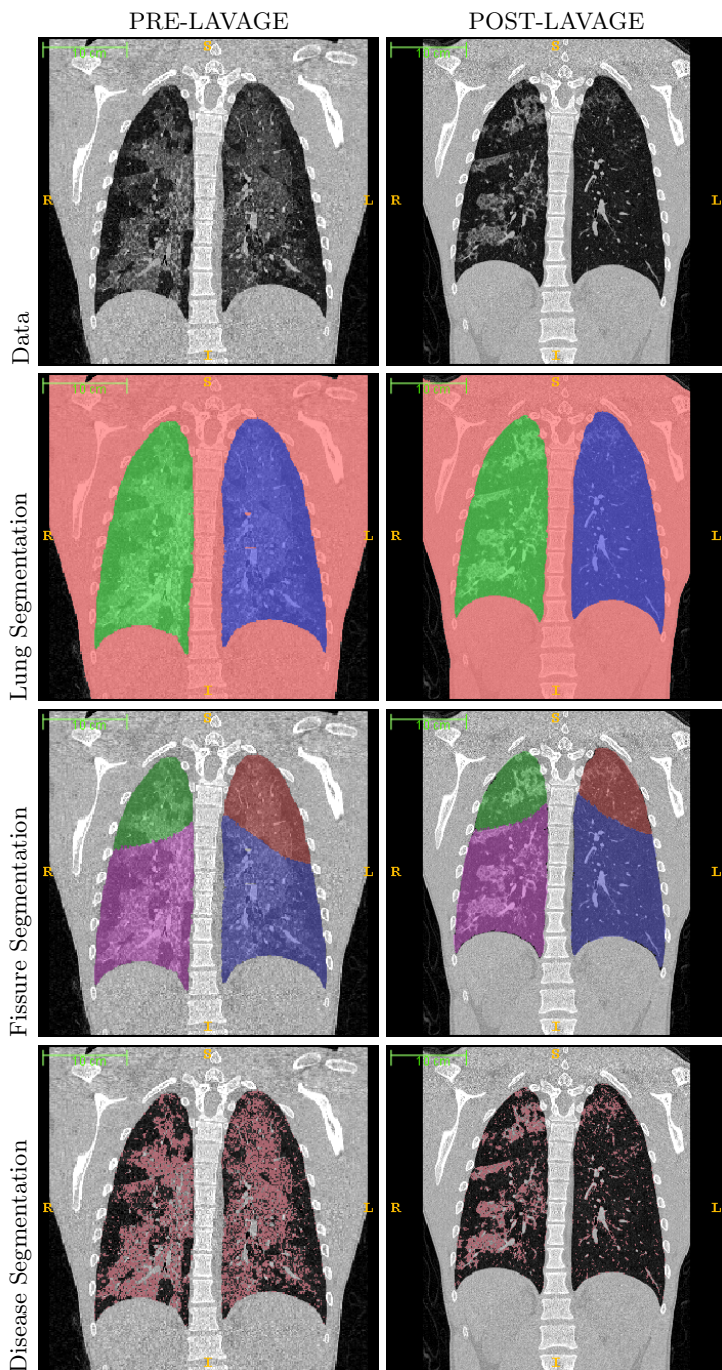


**Fig. 2.** The complete analysis algorithm illustrated using representative coronal sections from a PAP patient, pre- (left) and post-lavage (right). Details of each step can be found in section 2.

cross correlation similarity metric and Gaussian-regularized symmetric normalization (SyN) transformation model described in [10], which yields both the forward and inverse deformation fields after affine initialization.

### 2.3 Disease Segmentation Using Severity-Based Thresholds

Segmentation of regions of diseased lung is performed by empirically choosing thresholds based on the severity of the patient’s disease. Patients with less severe or less concentrated PAP intrinsically ventilate a higher percentage of their alveoli, and require thresholds closer to  $-1000$  Hounsfield units (HU), the attenuation of air, to segment alveolar deposits. Conversely, patients with extensive disease or very concentrated disease require thresholds closer to  $-100$  HU, an attenuation value between fat and water, since very little air mixes with the surfactant accumulating in their alveoli. For each of the five patients, thresholds were customized to the severity of their disease, as determined by visual inspection of the degree of alveolar infiltration. The same intensity thresholds were used for both the pre- and post-lavage images.

### 2.4 Analysis

Whole-lung and lobar volumes were computed from each patient’s image segmentations before and after WLL. Subsequently, the volume of disease in each lung was computed after the disease-specific thresholds were applied. The volumetric percentage of PAP in the lungs as a whole as well as in each lobe was then calculated, and pre- and post-lavage percentages were compared. Histogram analysis of the distribution of CT attenuation values in the lungs before and after treatment—normalized to the instantaneous lung volume during breath-holding—was also performed, with the expectation that after lavage, patients would demonstrate improved lung aeration, or an increased number of voxels closer to  $-1000$  HU.

## 3 Results

Patients A and B were classified as having moderate disease, because their alveolar deposits, though distributed throughout all lobes, were not extremely dense. Intensities in  $[-750, -300]$  HU were used to segment disease in these two patients. Patient C was noted to have focal, dense surfactant accumulation which, though it did not involve large portions of lung, was found to be extremely concentrated. Intensity thresholding in  $[-200, 0]$  HU was used for patient C, reflecting the high concentration of lipid (normally around  $-120$  HU). Patients D and E were classified as having severe disease, because their alveolar deposits were not only widespread in both lungs but also fairly dense. In these two patients, intensities in  $[-600, 0]$  HU best captured regions of disease.

Results of the pre- and post-lavage analysis are summarized in table 1. For each lobe of the lung and both lungs as a whole, we report the volume of disease

Region	Time	A	B	C	D	E
LUL	<i>pre</i>	0.31	0.63	0.10	0.16	0.49
	<i>post</i>	0.18	0.39	0.11	0.09	0.31
LLL	<i>pre</i>	0.47	0.39	0.09	0.24	0.64
	<i>post</i>	0.14	0.23	0.08	0.14	0.39
RUL	<i>pre</i>	0.23	0.41	0.13	0.15	0.18
	<i>post</i>	0.22	0.37	0.13	0.08	0.17
RML	<i>pre</i>	0.13	0.47	0.06	0.37	0.26
	<i>post</i>	0.11	0.29	0.07	0.21	0.18
RLL	<i>pre</i>	0.44	0.44	0.09	0.34	0.64
	<i>post</i>	0.27	0.27	0.09	0.19	0.47
Whole	<i>pre</i>	0.35	0.46	0.10	0.24	0.47
	<i>post</i>	0.19	0.30	0.10	0.13	0.33

**Table 1.** Summary of the global and lobar disease percentages (volume of disease in the region divided by total region volume) before and after WLL in patients A-E. LUL=left upper lobe, LLL=left lower lobe, RUL=right upper lobe, RML=right middle lobe, RLL=right lower lobe, Whole=both lungs.

in the region divided by the volume of the region itself before and after treatment. With the exception of patient C, who demonstrated nearly identical volumes of disease pre- and post-lavage, we quantify at least a 10% reduction in whole-lung disease in each patient, with decreases of up to 70% noted within individual lobes. As an example, 3-D renderings of disease distribution pre- and post-treatment for patient D (severe disease), are shown in figure 3.

Histograms of the CT attenuation in the lungs normalized to lung volume show that most patients who demonstrated a qualitative improvement in disease extent on CT experienced a leftward shift in parenchymal intensity distribution after lavage. This suggests a combination of factors: the expected improvement in lung aeration after removal of alveolar deposits as well as the ability to maintain a deeper inspiration post-treatment. Figures 4 and 5 demonstrate a marked leftward shift post-WLL in patient D, who had severe disease, both on a lobar level and over both lungs as a whole. These findings can be visually correlated with the 3-D renderings in figure 3. Comparatively, patient C, the patient with the dense though sparsely distributed areas of disease, did not appreciably respond to lavage, reflected both in the quantitative analysis (table 1) and in figure 6.

## 4 Discussion

The current clinical standard for assessment of disease in PAP is subjective analysis of increased or decreased alveolar involvement using serial CT over a patient's lifetime. In this work, we explore a quantitative approach to objectively

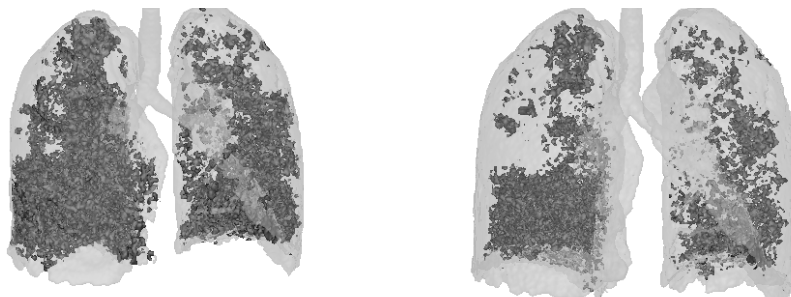


**Fig. 3.** 3-D volume renderings for patient D show the distribution of alveolar disease pre- (left) and post-lavage (right). Note the regions of increased aeration, particularly in the upper lobes, also reflected by the shift of parenchymal intensities towards  $-1000$  HU, or better ventilated lung.

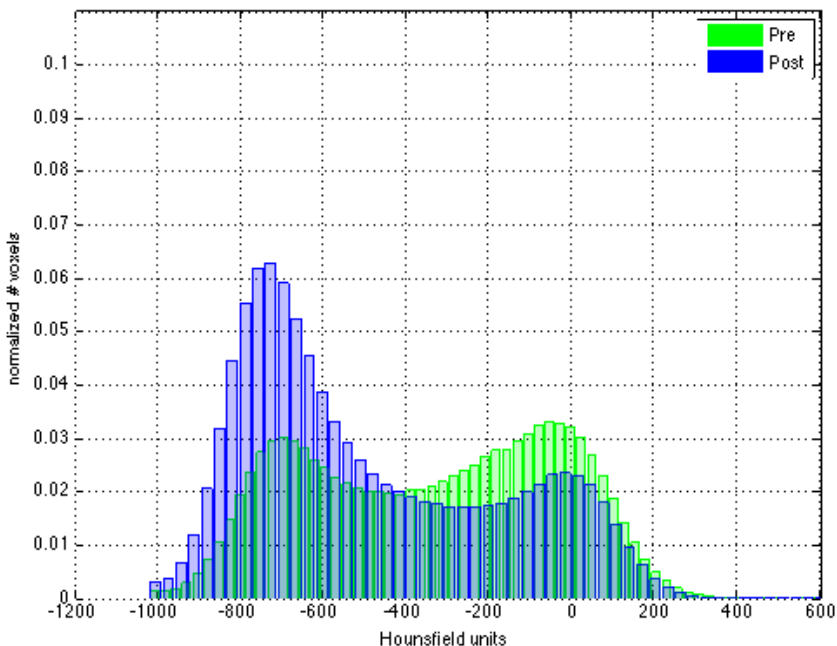


**Fig. 4.** Normalized histogram analysis of both lungs in patient D pre- and post-WLL demonstrates a leftward shift of parenchymal intensities (toward  $-1000$  HU, the attenuation of air) as alveolar deposits are removed from the lungs by lavage. In addition, patients may be able to sustain deeper inspirations during their CT studies as a result of treatment.

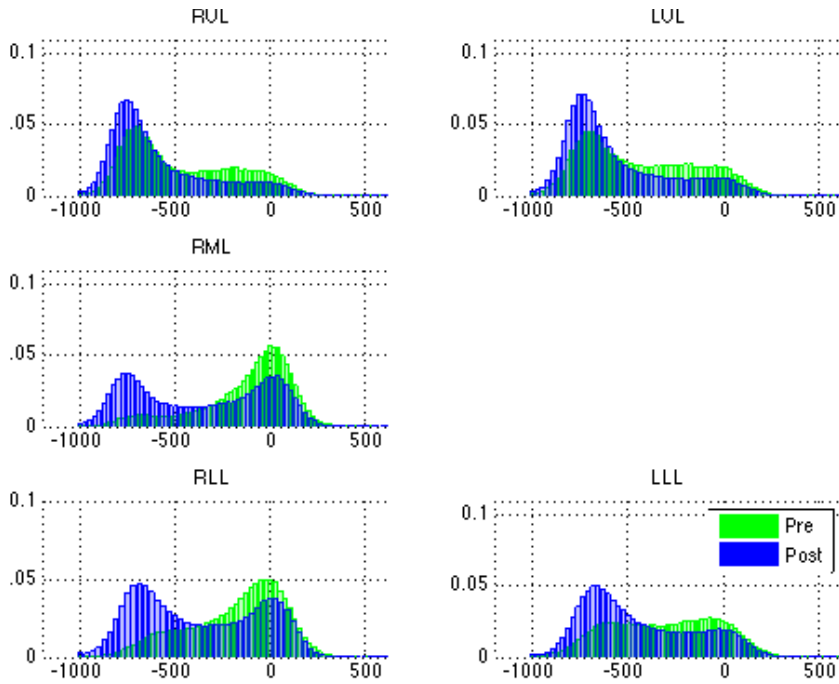


**Fig. 5.** Normalized lobar histogram analysis in patient D pre- and post-WLL similarly demonstrates a leftward shift of parenchymal intensities as alveolar deposits are washed from the lungs by lavage. Lobar identifications are described in table 1.

characterize the effects of WLL in five patients with PAP. We are able to regionally quantify the percentage of lung volume that is "recovered", i.e. depleted of excess surfactant, after saline lavage. This method has great potential clinical utility. It could assist pulmonologists in determining not only whether lavage has been effective, but also in regionally quantifying disease improvement as well as pinpointing areas of lung that are refractory to treatment and adjusting subsequent treatments accordingly. This methodology can further be applied in the realm of drug therapy for PAP, in order to evaluate the efficacy of pharmacologic agents under development and eventually to monitor patients' progress during treatment.

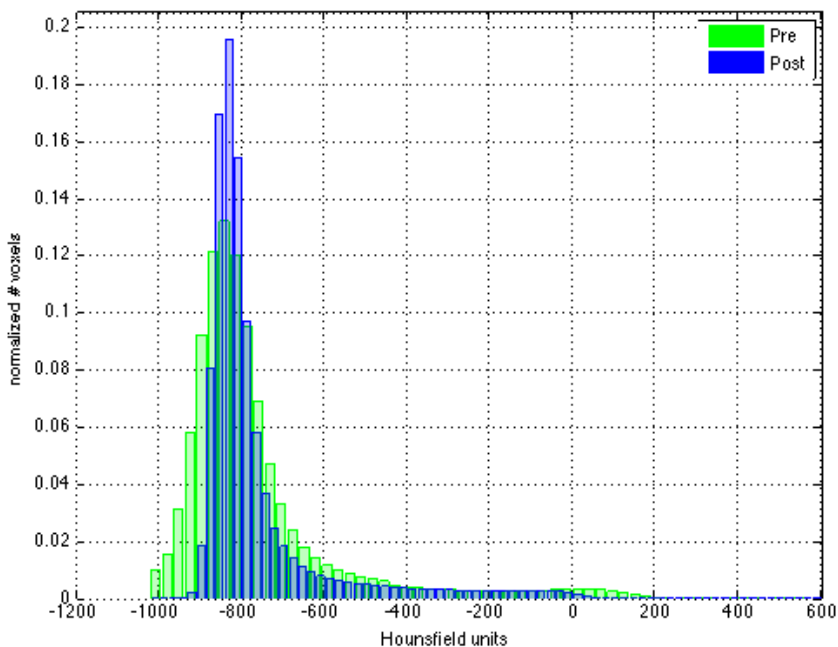


**Fig. 6.** Normalized histogram analysis of both lungs in patient C pre- and post-WLL does not reveal much response to treatment as compared to patient D in figure 4. Comparison of these normalized histograms can be used to assess treatment response within and across individuals.

However, there are limitations of this work that need to be addressed before this analysis can become an effective complement to patient care. In patients with widespread disease that involved sub-pleural lung (e.g., patient D), the initial automated segmentation failed to detect lung in regions of disease adjacent to the liver and chest wall. An improved initial segmentation that incorporates both intensity- and edge-based criteria would probably improve this step. Further-

more, automated lobar segmentation, instead of our semi-automated approach, would make the analysis timeline more realistically applicable to the clinical setting. However, the same challenge to the whole-lung segmentation also applies to fissure detection, and more work needs to be done to develop methods that can process this type of difficult data.

In preliminary experiments, we anticipated that a single range of intensities could be used to segment diseased lung in all patients with PAP. However, given the vast spectrum of disease and the combination of alveolar and interstitial patterns of disease that can be seen on CT with PAP, it became clear that thresholds needed to be customized to the individual patient. Future work will involve histogram manipulation for disease detection, so that intensity thresholds can be automatically extracted from the data to reflect the inherent severity of disease in the patient. In addition, we intend to validate our disease segmentation methodology using comparisons to manual segmentations of areas of disease performed by expert radiologists.

Lung volumes in the pre- and post-lavage studies are inherently different as patients are imaged at different times and may not breath-hold at the same volumes. In future analyses, we plan to incorporate registration of pre- and post-lavage datasets to eliminate this variable and generate a more accurate analysis of treatment efficacy.

This methodology can be applied to assess disease progression and response to treatment based on imaging findings in many pulmonary pathologies. These techniques would be particularly useful for infiltrative diseases such as idiopathic pulmonary fibrosis or a variety of chronic interstitial pneumonias that manifest with both interstitial and alveolar components. Furthermore, this work is an initial step towards enabling more quantitative reporting of clinical studies in radiology.

## References

1. Trapnell, B.C., Whitsett, J.A., Nakata, K.: Pulmonary alveolar proteinosis. *NEJM* **249**(26) (2003) 2527–2539
2. Ioachimescu, O.C., Kavuru, M.S.: Pulmonary alveolar proteinosis. *Chronic Respiratory Disease* **3**(3) (2006) 149–159
3. Beccaria, M., Luisetti, M., Rodi, G., Corsico, A., Zoia, M., Colato, S., Pochetti, P., Braschi, A., Pozzi, E., Cerveri, I.: Long-term durable benefit after whole lung lavage in pulmonary alveolar proteinosis. *Eur Respir J* **23**(4) (2004) 526–531
4. Lee, C.H.: The Crazy-paving Sign. *Radiology* **243**(3) (2007) 905–906
5. Holbert, J.M., Costello, P., Li, W., Hoffman, R.M., Rogers, R.M.: CT Features of Pulmonary Alveolar Proteinosis. *Am. J. Roentgenol.* **176**(5) (2001) 1287–1294
6. National Library of Medicine <http://www.itk.org>: Insight Segmentation and Registration Toolkit. (2003)
7. Hu, S., Hoffman, E., Reinhardt, J.: Automatic lung segmentation for accurate quantitation of volumetric X-ray CT images. *IEEE TMI* **20**(6) (2001) 490–498
8. Yushkevich, P.A., Piven, J., Hazlett, H.C., Smith, R.G., s. Ho, Gee, J.C., Gerig, G.: User-guided 3d active contour segmentation of anatomical structures: Significantly improved efficiency and reliability. *Neuroimage* (2006)

9. ANTS: Advanced normalization tools. <http://sourceforge.net/projects/advants>
10. Avants, B.B., Epstein, C.L., Grossman, M., Gee, J.C.: Symmetric diffeomorphic image registration with cross-correlation: evaluating automated labeling of elderly and neurodegenerative brain. *Med Image Anal* **12**(1) (Feb 2008) 26–41